Self-Assembly of Nanoparticle Ring Patterns*

Jürgen Parisi[a], Leonid V. Govor[a], Gottfried H. Bauer[a], and Günter Reiter[b]

[a] Department of Physics, University of Oldenburg, D-26111 Oldenburg, Germany
[b] Institut de Chimie des Surfaces et Interfaces, CNRS-UHA, 68057 Mulhouse Cedex, France

Reprint requests to Prof. J. P.; E-mail: parisi@ehf.uni-oldenburg.de

Z. Naturforsch. **61a,** 99 – 102 (2006); received December 8, 2005

We focus on the formation of self-assembled micrometer-sized rings of $CoPt_3$ nanoparticles due to phase separation of a binary solution, giving rise to a bilayer structure and subsequent decomposition of the top layer into droplets. Evaporation of the remaining solvent from the droplet leads to a shrinking of its contact line. The nanoparticles located at the contact line follow its motion and self-assemble along the line accordingly.

Key words: Nanoparticles; Self-Assembly; Phase Separation.

1. Introduction

During drying of liquid coffee droplets on a solid substrate, ring-like deposits remain along the perimeter, an observation standing for an ubiquitous phenomenon reported previously for macro-sized structures [1, 2]. According to Deegan et al. [2] on the ring formation in an evaporating droplet, two effects become important: contact line pinning and predominant evaporation at the edge of the droplet. When the contact line is pinned, an outward flow J_f of the solvent develops, since the solvent removed via evaporation from the edge of the droplet must be replenished by J_f from the interior, which may transfer up to 100% of the solute to the contact line [2].

In the present work, we demonstrate that a ring of nanoparticles at the edge of an evaporating micron-size droplet has been formed not as a consequence of the action of the flow J_f, but rather as a retraction of the droplet contact line during evaporation: nanoparticles located at the contact line follow its motion and self-assemble along the latter.

2. Experimental

In our experiments, we have used a blend (B) that contains 50% of a 1% nitrocellulose solution (NC) in amyl acetate and 50% of a $CoPt_3$ particle solution in hexane (17 mg/ml) with hexadecylamine (HDA) acting as stabilizer (7 mg/ml) [3]. The thin films were prepared during the wetting process of a binary mixture on a water surface [4]. After drying, the thin films were transferred onto glass substrates, where their topography was analyzed by atomic force microscopy (AFM, model Burleigh Vista 100). The arrangement of the $CoPt_3$ particles has been studied by transmission electron microscopy (TEM, model Zeiss EM 902).

3. Results

On top of the cellulose thin film, we disclosed a droplet-like phase separated pattern of HDA. The height of the isolated droplets, h_d, varied from 5 to 23.5 nm across the entire diameter of the spreading film from the center to its edge. The corresponding diameter of the droplets, D_d, varied from 0.6 to 1.5 μm. Figures 1a and b show an AFM image of a structure of the HDA droplets with $h_d = 15$ nm and $D_d = 950$ nm. For determination of the spatial distribution of the droplets in the cellulose film, the HDA droplets were removed by immersing the specimen in hexane for 5 min. The thickness of the underlying cellulose film was more or less constant at about 3 – 4 nm. The depth of the voids that remained in the cellulose film after removal of the HDA droplets amounted to about 1 nm. These results indicate that the HDA droplets do not have any contact to the substrate surface. The TEM analysis of the droplet patterns clearly demonstrates that the $CoPt_3$ particles with radius 3 nm self-assemble into a ring located at the edge of the HDA droplet. Figures 1c and d display particle rings

* Paper presented at the XVII Latin American Symposium on Solid State Physics, La Habana, December 6 – 9, 2004.

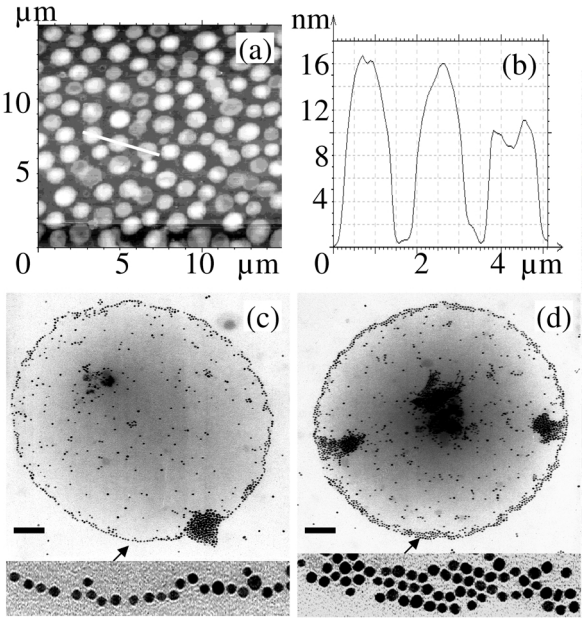

Fig. 1. (a) AFM image of HDA droplets on a cellulose film with average diameter $D_d = 950$ nm and average height $h_d = 15$ nm. (b) AFM profile analysis of the scan line indicated in (a). (c) and (d) show TEM images of $CoPt_3$ particle rings formed at the edge of HDA droplets. (c) 1D assembling; scale bar 100 nm. (d) 2D assembling; scale bar 110 nm. The detailed structure of the rings is magnified in the insets.

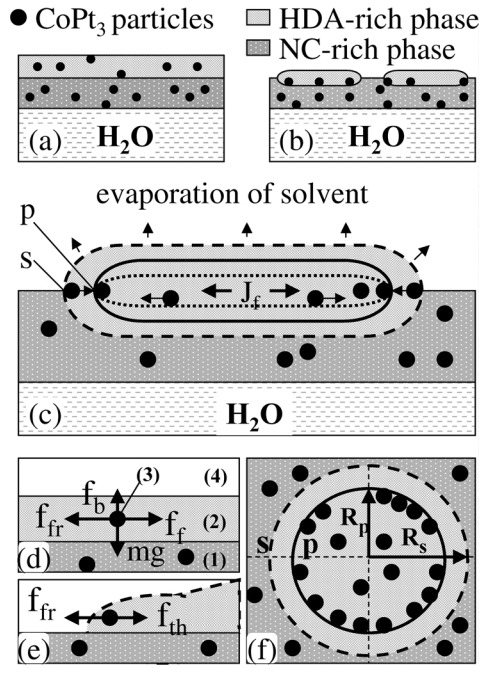

Fig. 2. Schematic illustration of the development of the phase-separated structure and the corresponding $CoPt_3$ particle rings. (a) Formation of phase-separated layers. (b) Rupture of the HDA-rich layer into droplets. (c) Formation of the particle ring in a separated HDA-rich droplet. The contact line moves from point s to point p before it is fixed; J_f indicates the radial outward solvent flow. (d) Forces which act on the $CoPt_3$ particle in the interior of the HDA droplet. (e) Forces which act on the $CoPt_3$ particle located at the contact line of the HDA droplet. f_{th} is the thickening force per particle. (f) Assembling of the particles at the contact line during its motion; R_s is the droplet radius developing immediately after the rupture of the HDA-rich layer; R_p is the radius of the dry HDA droplet.

with diameter 860 nm and 930 nm. Note that Figs. 1c and d have been recorded before and after removal of the HDA droplets from the sample, and both number and position of the individual $CoPt_3$ particles did not change. That means that these particles are located on the cellulose layer and are mainly embedded therein.

In Fig. 2, we sketch our idea for a possible mechanism of the ring formation. In accordance with the experimental results, we assume that the initial thin solution layer on the water surface transforms into a bilayer which consists of a hexane/hexadecylamine-rich (HDA-rich) phase with thickness ≤ 300 nm at the solution-air interface and an amyl acetate/cellulose-rich (NC-rich) phase with thickness ≤ 300 nm at the solution-water interface (Fig. 2a). The thickness of both layers was determined from the volume ratio of the two phases in the initial blend solution. The number of $CoPt_3$ particles in each layer was about 6×10^{12}. The formation of the bilayer may be attributed at least to the fact that the HDA-rich phase with its lower surface free energy (surface tension $\gamma_{HDA/A} = 18.4$ mN/m for the HDA-rich layer and $\gamma_{NC/A} = 24.6$ mN/m for the NC-rich layer) enlarges at the surface region, in order to minimize the free energy at the interface between air and solution [5]. The equilibrium thickness d_e of the wetting HDA-rich layer on the NC-rich layer results from a competition between long-range forces (as measured by $\gamma_{HDA/A}$ with the tendency to thicken the film) and spreading (as measured by the wetting coefficient $S_{HDA/NC}$ with the tendency for film thinning) [6, 7]. The HDA-rich layer will decompose into droplets when the layer thickness d is sufficiently smaller than d_e (by about $10-15\%$) [8]. Below this critical value, the HDA-rich layer gets unstable against nucleation and growth of the dry patches occurs, in order to achieve the equilibrium thickness d_e, and the layer decomposes into droplets [7] (see Fig. 2b). We assume that during the decomposition

process the thickness d_e was in order of the nanoparticle diameter. It follows from the fact that all nanoparticles shown in Figs. 1c and d are rather located on the interface between the HDA droplet and the cellulose layer, but not in the other part of the HDA droplet. If the particles were not partially embedded in the cellulose layer, they would have been washed off during HDA removal. As far as the contact line in the HDA-rich droplet (interface between air, liquid, and substrate) is not fixed, a spatially uniform evaporation occurs, and the interface moves towards the center of the droplet (from the dashed to the solid line in Fig. 2c). Those nanoparticles that are located at the contact line follow its shrinking and, consequently, assemble in a ring-like structure. When the contact line is fixed (point p in Fig. 2c), the interface moves from the solid to the dotted line, and an outward flow J_f of the solvent develops [1, 2].

We compare the number of $CoPt_3$ particles assembled at the contact line during its motion with the number of particles which move with the flow J_f in outward direction: the motion of a $CoPt_3$ particle in a fluid HDA-rich droplet via the flow J_f can be qualitatively estimated by the force equation $f_f = f_{fr}$, where other contributions, e.g., gravity force ($mg = 2.2 \times 10^{-20}$ N) and buoyancy force ($f_b = 2.6 \times 10^{-21}$ N), are negligible compared to the flow force $f_f = 6\pi\eta r_s v$ and the friction force f_{fr}, see Figure 2d. Here, $\eta = 5.9 \times 10^{-4}$ Ns/m^2 and v are viscosity and velocity of the flow J_f, respectively; $r_s = r + \delta = 4.4$ nm is the radius of the $CoPt_3$ particle overcoated with a HDA monolayer (with thickness $\delta = 1.4$ nm). The counterpart $f_{fr} = K f_z$ is a lateral friction force acting on the particle, where K is a dimensionless coefficient of the order unity [8] and f_z is the dispersional attraction along the vertical axis between particle and NC-rich layer. The interaction energy between a small $CoPt_3$ particle and the NC-rich layer can be described as $W(D) = -Ar/6D$ [9], and the corresponding interaction force reads $f_z = \partial W(D)/\partial D = Ar/6D^2$, where D gives the distance between the particle and the NC-rich layer, and A denotes the Hamaker constant [10]. Here, the thickness of the HDA layer (2) in Fig. 2d between the $CoPt_3$ particle (3) and the NC-rich layer (1), and that between the $CoPt_3$ particle and air (4) is very small, and accordingly, all interaction components between the surrounding materials across the $CoPt_3$ particle will contribute to its total interaction energy [11]. From standard arguments, the interaction force between the $CoPt_3$ particle and the NC-rich layer across the HDA layer can be approximated by [9]

$$f_z = \frac{r}{6}\left[\frac{A_{232}}{(2r)^2} - \frac{\sqrt{A_{121}A_{323}}}{(2r+\delta)^2} - \frac{\sqrt{A_{424}A_{323}}}{(2r+\delta)^2} + \frac{\sqrt{A_{424}A_{121}}}{(2r+2\delta)^2}\right]. \quad (1)$$

The effective Hamaker constants A_{232}, A_{121}, A_{323}, and A_{424} can be composed by the respective Hamaker constants of each medium [12], $A_{232} = A_{323} = \left(\sqrt{A_{22}} - \sqrt{A_{33}}\right)^2$, $A_{121} = \left(\sqrt{A_{11}} - \sqrt{A_{22}}\right)^2$, $A_{424} = \left(\sqrt{A_{44}} - \sqrt{A_{22}}\right)^2$. The individual Hamaker constants A_{ii} are to be extracted from the surface tension γ_{ii} as $A_{ii} = 24\pi\gamma_{ii}(D_o)^2$ with a cutoff intermolecular separation $D_o = 0.165$ nm [9]. The latter equation yields $A_{22} = 5.3 \times 10^{-20}$ J for the experimentally obtained value $\gamma_{HDA/A} = 25.8$ mN/m, taken from the Zisman plot measured on the solid HDA film [13]. For the NC-rich layer with $\gamma_{NC/A} = 24.6$ mN/m at the moment of the dewetting HDA-rich layer, the corresponding Hamaker constant amounts to $A_{11} = 5.0 \times 10^{-20}$ J. Considering the characteristic Hamaker constant for most metals [9] (and accordingly for $CoPt_3$, as well), $A_{33} \approx 4 \times 10^{-19}$ J and $A_{44} = 0$, the effective Hamaker constants $A_{232} \approx 1.6 \times 10^{-19}$ J, $A_{121} \approx 0.4 \times 10^{-22}$ J, $A_{424} \approx 5.3 \times 10^{-20}$ J could be determined. For the above values attributed to the parameters in (1), the calculated interaction force becomes $f_z \approx 1.3 \times 10^{-12}$ N. Assuming $K \approx 0.5$ [8], the friction force is quantified to $f_{fr} \approx 6.6 \times 10^{-13}$ N. From the balance $f_f = f_{fr}$, the velocity v of the flow J_f necessary to move the $CoPt_3$ particle from the interior to the contact line would get $v \approx 6.7 \times 10^3$ µm/s.

So far, no experimental results on the flow velocity in droplets of micron-sized diameters are available. For macro-sized droplets on solid substrate, Deegan et al. [2] have measured the velocity of polysterene spheres with diameter 1 µm in a drying water droplet with a radius of 2 mm, after the contact line has been pinned, to about 6 µm/s. The evaporation rate of water in the diffusion-limited regime was proportional to the diameter of the droplet, as a consequence of the finite probability for evaporating molecules to return to the liquid state [14]. In our case, the velocity of the flow J_f in micron-sized HDA-rich droplets must be substantially smaller than 6 µm/s, and the value $v \approx 6.7 \times 10^3$ µm/s cannot be established.

According to these results, we assume that practically all $CoPt_3$ particles in a ring are assembled due to

the retraction of the contact line caused by evaporation. The force acting radially on the contact line and aiming at thickening the HDA-rich droplet is given by [7]

$$F_{\mathrm{th}} = 2\pi R S_{\mathrm{HDA/NC}}((d_{\mathrm{e}}/d)^2 - 1), \tag{2}$$

where R denotes the radius of the fluid HDA-rich droplet. The force F_{th} drags the $CoPt_3$ particles with the retraction of the droplet contact line until it is balanced by the total friction force F_{fr}, see Figs. 2e and f. The force F_{fr} results from the superposition of the friction forces of individual particles, located at the contact line of a droplet with radius $R = R_{\mathrm{p}}$, and can be formulated via the friction force per particle, $f_{\mathrm{fr}} = K f_z$ [see (1)]:

$$F_{\mathrm{fr}} = K f_z \phi (R_{\mathrm{s}}^2 - R_{\mathrm{p}}^2)/r_{\mathrm{s}}^2, \tag{3}$$

where ϕ means the area fraction covered by particles. The expected value $\phi = 126 \times 10^{-3}$ was derived from the concentration of particles in the initial blend solution. Experimentally, from the particle concentration in the interior of the rings illustrated in Figs. 1c and d, we have found that ϕ amounts to 23×10^{-3} and 48×10^{-3}, respectively. The radius R_{p} has to be extracted from (2) and (3) as

$$R_{\mathrm{p}} = \frac{1}{2}\left\{\left[\frac{2\pi r_{\mathrm{s}}^2 S_{\mathrm{HDA/NC}}((d_{\mathrm{e}}/d)^2 - 1)}{K f_z \phi}\right]^2 + 4R_{\mathrm{s}}^2\right\}^{1/2} - \frac{\pi r_{\mathrm{s}}^2 S_{\mathrm{HDA/NC}}((d_{\mathrm{e}}/d)^2 - 1)}{K f_z \phi}. \tag{4}$$

The validity of (4) can be checked with the rings shown in Figs. 1c and d, the number $N_{\mathrm{d}} = 131$ of which was observed on the sample with an area $A_{\mathrm{s}} = 18.2 \times 21.4\ \mu\mathrm{m}^2$. From these data, the value $R_{\mathrm{s}} = (A_{\mathrm{s}}/4N_{\mathrm{d}})^{0.5} = 860$ nm is estimated. The predominant parameters in (4) are $S_{\mathrm{HDA/NC}}$, d, and K. With $S_{\mathrm{HDA/NC}} = 0.25$ mN/m, $d = 0.85 d_{\mathrm{e}}$ [8], and $K = 0.5$ [8], the corresponding radius R_{p} calculated from (4) for the ring shown in Fig. 1c becomes 560 nm. The experimentally measured $R_{\mathrm{p}} = 430$ nm may be reproduced via (4) by introducing $d = 0.85 d_{\mathrm{e}}$, $K = 0.5$, and $S_{\mathrm{HDA/NC}} = 0.42$ mN/m instead of 0.25 mN/m. That means, a small variation of $S_{\mathrm{HDA/NC}}$ can lead to large changes of R_{p} in (4). The corresponding value of R_{p} of the ring shown in Fig. 1d, derived from (4) with $S_{\mathrm{HDA/NC}} = 0.42$ mN/m, $d = 0.85 d_{\mathrm{e}}$, and $K = 0.5$, is 600 nm (experimentally, $R_{\mathrm{p}} = 465$ nm). Obviously, the above agreement between the experimentally measured and theoretically calculated values of R_{p} supports our model that $CoPt_3$ particle rings were formed by the retraction of the contact line of the HDA droplet during evaporation.

4. Conclusions

In summary, we have experimentally demonstrated that phase separation in a binary solution leads to the formation of a bilayer structure. The solvent evaporation from the bilayer leads to the decomposition of the top HDA-rich layer into micron-sized droplets. The subsequent evaporation of such droplets gives rise to a shrinking of their contact line. The $CoPt_3$ particles located at the contact line follow its motion, and assemble along that.

Acknowledgement

The authors would like to thank E. Shevchenko and H. Weller for preparation of $CoPt_3$ nanoparticles and for valuable discussions of the experimental results.

[1] E. Adachi, A. S. Dimitrov, and K. Nagayama, Langmuir **11**, 1057 (1995).
[2] R. D. Deegan, O. Bakajin, T. F. Dupont, G. Huber, S. R. Nagel, and T. A. Witten, Phys. Rev. E **62**, 756 (2000).
[3] E. Shevchenko, D. Talapin, A. Kornowski, A. Rogach, and H. Weller, J. Am. Chem. Soc. **124**, 11480 (2002).
[4] L. V. Govor, I. A. Bashmakov, R. Kiebooms, V. Dyakonov, and J. Parisi, Adv. Mater. **13**, 588 (2001); L. V. Govor, G. H. Bauer, G. Reiter, E. Shevchenko, H. Weller, and J. Parisi, Langmuir **19**, 9573 (2003).
[5] F. Bruder and R. Brenn, Phys. Rev. Lett. **69**, 624 (1992); U. Steiner, J. Klein, and L. J. Fetters, Phys. Rev. Lett. **72**, 1498 (1994).
[6] P. G. de Gennes, Rev. Mod. Phys. **57**, 827 (1985).
[7] F. Brochard-Wyart and J. Daillant, Can. J. Phys. **68**, 1084 (1990).
[8] P. C. Ohara and W. M. Gelbart, Langmuir **14**, 3418 (1998).
[9] J. N. Israelachvili, Intermolecular and Surface Forces, Academic Press, London 1991.
[10] H. C. Hamaker, Physica **9**, 1058 (1937).
[11] G. Reiter, A. Sharma, A. Casoli, M.-O. David, R. Khanna, and P. Auroy, Langmuir **15**, 2551 (1999).
[12] J. Visser, Adv. Colloid Interface Sci. **3**, 331 (1972).
[13] W. A. Zisman, Contact Angles, Wettability, and Adhesion, ACS Adv. Chem. Ser. **43**, 1991.
[14] J. T. Davies and E. K. Rideal, Interfacial Phenomenon, Academic Press, New York 1963.